Wind Engineering Joint Usage/Research Center
FY2019 Research Result Report

Research Field: Wind hazard mitigation and wind resistant design
Research Year: FY2019
Research Number: 193003
Research Theme: Research on Proper Orthogonal Decomposition (POD) of wind pressures on hip-roof buildings

Representative Researcher: Qingshan, Yang

Budget [FY2019]: 450,000Yen

*There is no limitation of the number of pages of this report.
*Figures can be included to the report and they can also be colored.
*Submitted reports will be uploaded to the JURC Homepage.

1. Research Aim

Traditional Chinese roofs have some special features, including curved slopes, high ridges and double eaves, which are different from conventional linear-sloped roofs. In order to investigate wind pressure characteristics acting on traditional Chinese roofs, wind tunnel tests are carried out in a boundary layer wind tunnel in Beijing Jiaotong University. To explain how the wind flow acting on the traditional Low-rise building, the method of Proper Orthogonal Decomposition (POD) would be adopted to analyze the wind pressures on traditional roofs. However, because of the wind tunnel facilities, wind speeds of the incoming flow and the wind pressures on the tested models couldn't be measured simultaneously in Beijing Jiaotong University. Thus the analyses of the correlation between the principle coordinate from Proper Orthogonal Decomposition (POD) and the incoming wind speed has been limited. To get more efficient data in TPU WERC, this research is aim to measure the wind pressures on Chinese traditional building models as well as the wind speeds of the incoming flow.
To illustrate more clearly, wind pressures characteristics on a flat-roof building model and a high-rise building model, which have known clearly and widely, have also been tested and analyzed. Corresponding results have been shown in the section 3.

2. Research Method

Proper orthogonal decomposition usually implies for the Karhunen-Loeve decomposition (Lumley, 1970). Multi-variate spatially-correlated random pressure field can be expressed by following optimum approximation, in which this pressure field is expand into a sum of products of time-independent basic orthogonal vectors and time-dependent uncorrelated random processes as follows:

$p(\upsilon,t)=x(t)^{T}\varphi(\upsilon)=\sum_{j=1} x_j(t)\varphi_j(\upsilon)$

where $x_j(t)$: j-th principal coordinate as univariate zero-time random processes, $E[x_j(t)]=0$;$\varphi_j(\upsilon)$: j-th basic orthogonal vector, $\varphi_j(\upsilon)^{T}\varphi_j(\upsilon)=\delta_{ij}$ (δ_{ij} : Kronecker delta); $x(t)=\{x_1(t), x_2(t), \dots, x_N(t)\}$; $\varphi(\upsilon)=\{\varphi_1(\upsilon), \varphi_2(\upsilon), \dots, \varphi_N(\upsilon)\}$. It is also notable that eigenvalues gained from this eigenvalue solution usually reduce fast, accordingly, only very few number of low-order eigenvectors associated with low-order high eigenvalues can obtain optimum approximation and describe the whole random process.
The covariance matrix-based orthogonal vectors are found as the eigenvector solutions of the zero-time-lag covariance matrix R_p of the N-variate random pressure field p(t):

$R_p\Theta_p=\Gamma_p\Theta_p$

where $\Gamma_p=\mathrm{diag}(\gamma_{p1}, \gamma_{p1}, \dots, \gamma_{pN})$, $\Theta_p=\{\theta_{p1}, \theta_{p1}, \dots, \theta_{pN}\}$: covariance eigenvalue and eigenvector (covariance mode) matrix.
Similarly, the spectral eigenvalues and eigenvectors are found based on to the eigenvalue problem of the cross spectral matrix $S_p(n)$ of random pressure process p(t):

$S_p(n)\Psi_p(n)= \Lambda_p(n)\Psi_p(n)$
Where $\Lambda_p(n)=diag(\lambda_{p1}(n), \lambda_{p2}(n), \dots, \lambda_{pN}(n))$,$\Psi_p(n)=[\psi_{p1}(n), \psi_{p2}(n), \dots, \psi_{pN}(n)]$: spectral eigenvalue and eigenvector (spectral mode) matrix.

3. Research Result

Wind tunnel tests on the flat-roof building model, gable-roof building model, hip-roof building model and high-rise building model has been carried out in the large scale wind tunnel in TPU WERC. The POD results of flat-roof building model and high-rise building model have been shown here.

3.1 Covariance and Spectral Proper Orthogonal Decompositions of Wind Pressure Fields on Low-Rise Building

3.1.1 Wind tunnel experiments

Wind pressure measurements of a low-rise building were carried out in the Tokyo Polytechnic University's open-circuit wind tunnel. The power-law exponent α is approximated as 0.15. The mean wind speed U_H at model height is 8.5m/s. The sampling frequency is 1000Hz. And the geometric scale is 1/100. The wind pressures of the 7th column were selected to investigate the proper orthogonal decomposition based on the covariance and spectral matrix.

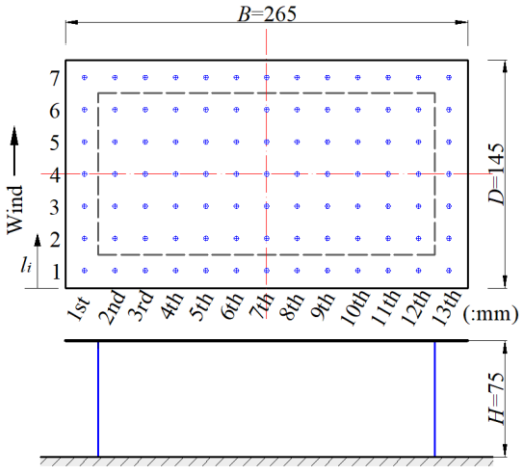

Fig. 1 Experimental model

3.1.2 Surface pressure distribution and bluff body flow pattern

When the wind direction is paralleled to the roof depth. The wind pressures on the symmetric axis is with the certain mechanism of columnar vortex, regarding to only one dominant mechanism. Covariance POD and spectral POD can be compared by decomposing the wind pressures of Point 1~7. Mean C_p, RMS C_p and the power spectrum density are shown in Fig.2 and Fig.3, they will be used later to check the loading modes and the principle coordinates.

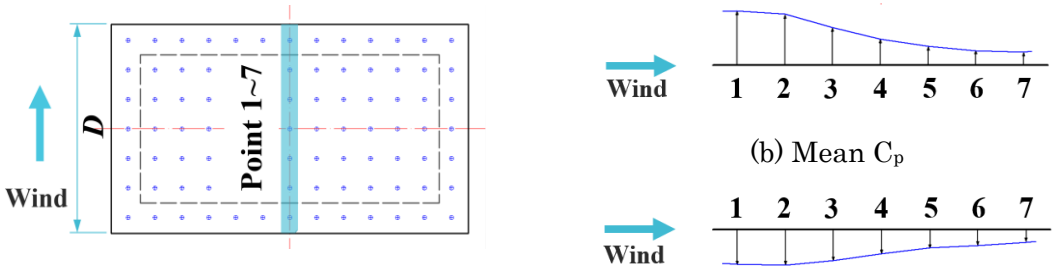

(a) Pressure points (b) Mean C_p (c) RMS C_p

Fig. 2 Mean and fluctuating wind pressure coefficients

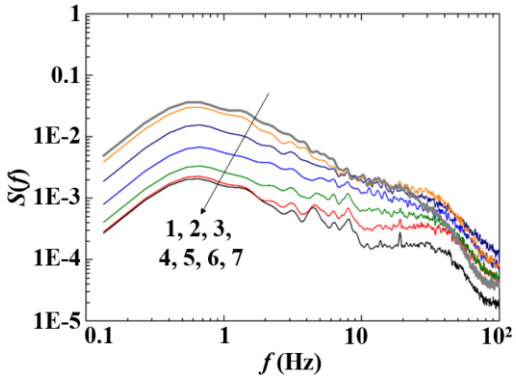

Fig. 3 PSD of the fluctuating wind pressure coefficients

3.1.3 Covariance matrix-branched proper orthogonal decomposition

Firstly Covariance POD is used to decomposing the wind pressure field. According to the energy contribution of each covariance mode (Fig. 4), the first mode is with 48% contribution, the second mode is with 22% contribution, the cumulative contribution of the first two modes is 70%. From the eigenvectors (Fig. 5), the first mode is similar to the distribution of the RMS C_p as shown in Fig. 2(c); the second mode indicates the contribution of the pressure of the first three point on the windward side; the third the forth modes are complicated and can be neglected considering the small contribution.

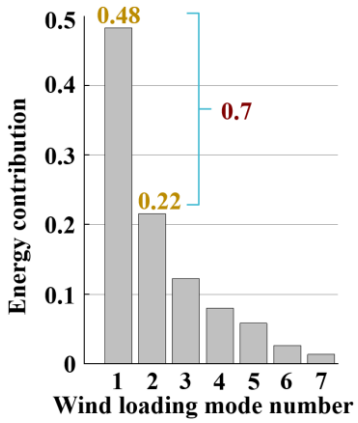

Fig. 4 Energy contribution of each covariance mode

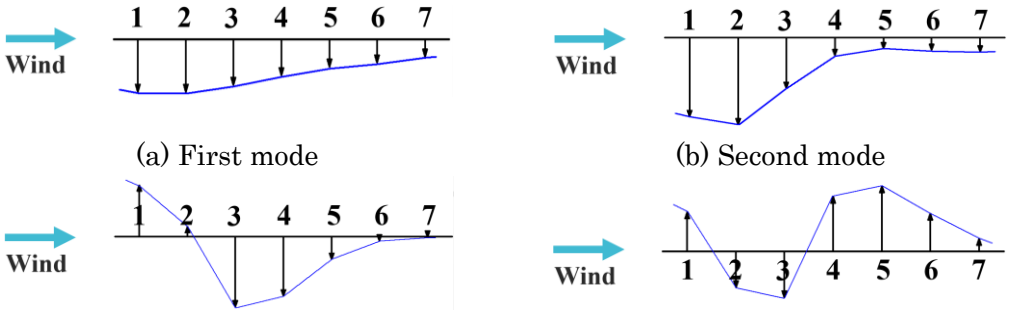

(a) First mode (b) Second mode

(c) Third mode (d) Forth mode

Fig. 5 First four covariance modes of experimental model

From the covariance principle coordinate (Fig. 6(a)), the first and second covariance principle coordinates express the considerable amplitudes, others are small. In the aspect of the power spectrum (Fig. 6(b)), the first covariance coordinate contains large energy in the low frequency range and decrease fast in the high frequency range, just like the pressure power spectrum at Point 1.

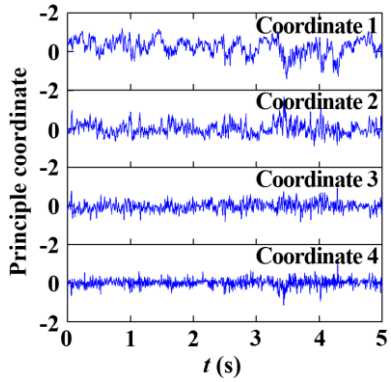

(a) Time history of covariance principle coordinate

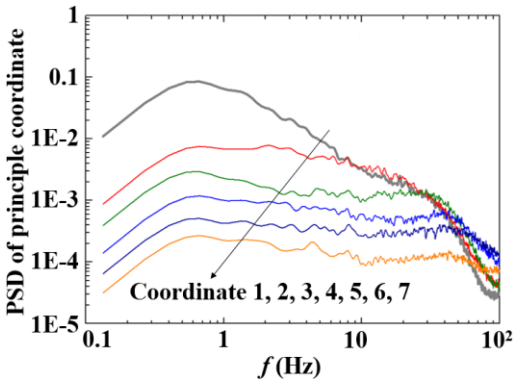

(b) PSD of covariance principle coordinate

Fig. 6 Covariance principle coordinate

The original pressure fields at Point 1 can be reconstructed by using limited number of the low-order covariance modes. Fig. 7 shows that, the first covariance mode isn't enough for reconstructing the original pressure time history and the power spectrum. However, the first two covariance mode are almost enough for reconstructing the original pressure time history and the power spectrum.

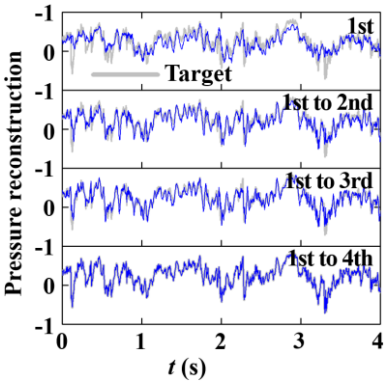

(a) Recostructed time history of P1

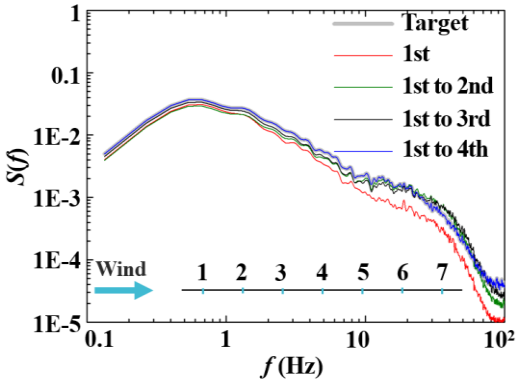

(b) Reconstructed PSD of P1

Fig. 7 Reconstructed pressure of P1 from covariance POD

3.1.4 Spectral matrix-branched proper orthogonal decomposition

Frequency-dependent spectral eigenvalues and spectral eigenvectors can be solved out from frequency-dependent cross spectral matrix of the random pressure field.

Fig. 8 shows the first six spectral eigenvalues. The first spectral eigenvalues exhibit much dominantly than the others. The energy contribution of the spectral mode (Fig. 9) can be calculated by integrating the spectral eigenvalues of each mode. As the results, the first spectral mode energy contribution is 72%, which is almost equal to the first two covariance modes.

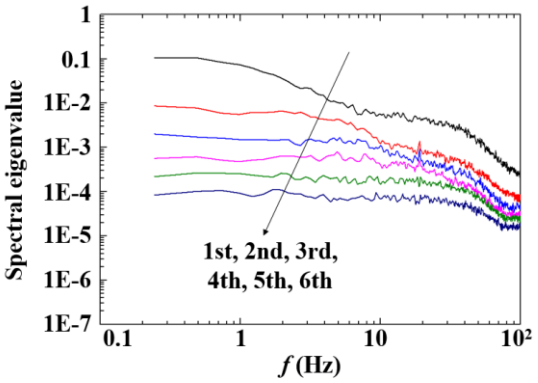

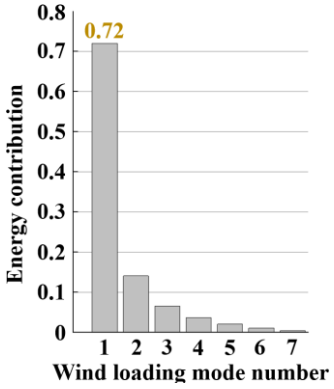

Fig. 8 First six spectral eigenvalues

Fig. 9 Energy contribution of each spectral mode

From the spectral principle coordinate (Fig. 10), the first spectral coordinate is dominant, while others contains lower amplitudes.
The first three spectral modes (Fig. 11) has been shown that, the first spectral mode is similar to the point pressure power spectrum. From Point 1 to 7, the energy in the low frequency range become lower and lower. In the high frequency, the energy of Point 1 is the lowest. The second and third spectral modes are complicated, corresponding to the lower energy contribution.

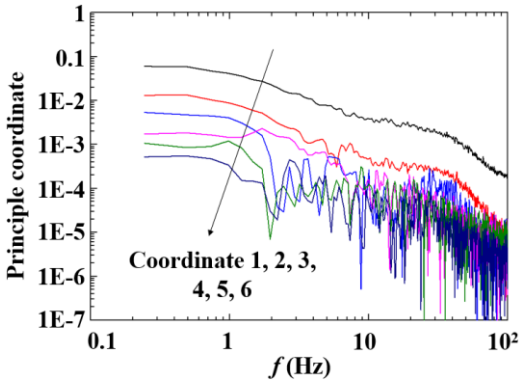

Fig. 10 Spectral principle coordinate

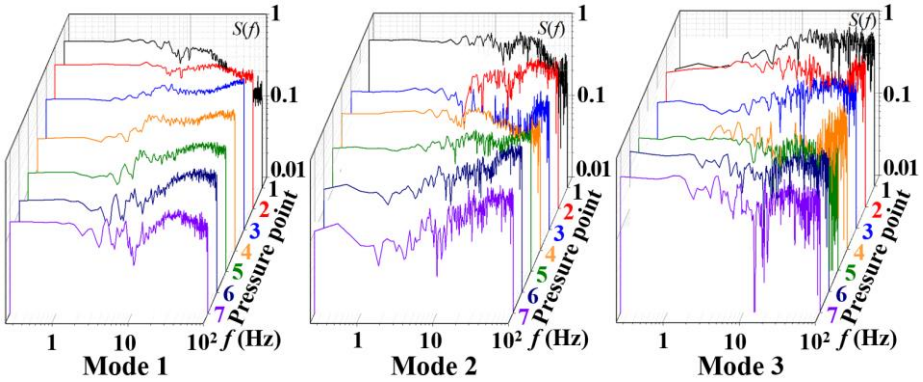

Fig. 11 Spectral mode

Reconstructing the power spectrum at Point 1 by using the spectral principle coordinate as shown in Fig. 12. It can be deduced, the first spectral mode matches the original power spectrum well at all frequency range. Considering the first two modes, the accuracy has quite limited increasing.

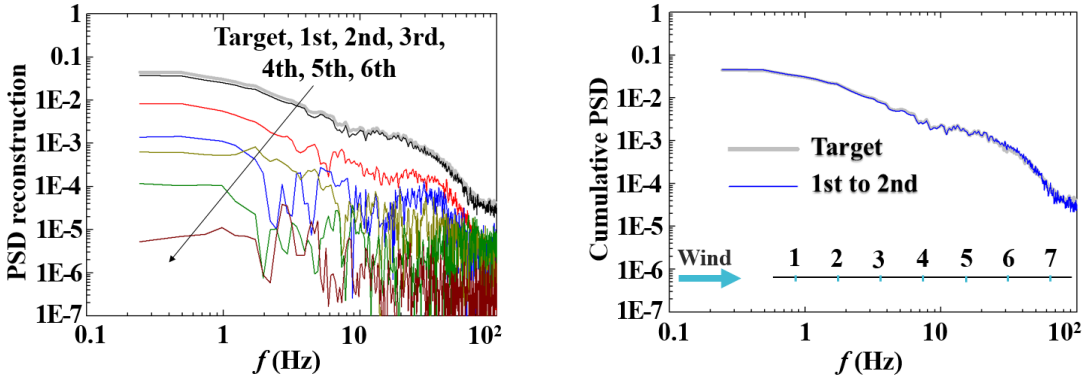

(a) Reconstructed power spectrum of each spectral mode

(b) Reconstructed power spectrum of cumulative spectral modes

Fig. 12 Reconstructed spectrum of P1

3.2 Covariance and Spectral Proper Orthogonal Decompositions of Wind Pressure Fields on Low-Rise Building

3.2.1 Wind tunnel experiments

Wind pressure measurements of a high-rise building were carried out in the Tokyo Polytechnic University's open-circuit wind tunnel.

The wind pressures of the 7th layer were selected to investigate the proper orthogonal decomposition based on the covariance and spectral matrix. The power-law exponent α is approximated as 0.28. The mean wind speed U_H at model height is 10.5m/s. The sampling frequency is 1000Hz. And the geometric scale is 1/400.

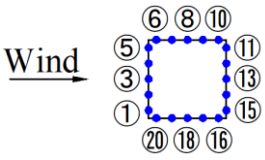

7th layer pressure point

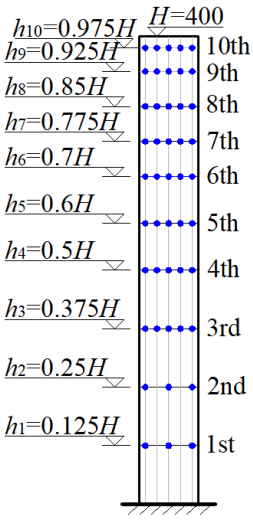

Fig. 13 Experimental model

3.2.2 Surface pressure distribution and bluff body flow pattern

Fluctuating pressure distributes steadily on each side. The power spectra of the fluctuating pressures shows that, the peak frequencies at 11Hz are observed on the sideward and the edge of the leeward side. It is explained that the Karman vortex formed and shed at the wake of model. Shedding frequency depends on the Strouhal number (S_t) of the cross section. To compare with the principle coordinate, drag force, lift force and their power spectrum are listed in Fig. 16. And the power spectrum of lift force has a peak corresponding to the vortex shedding.

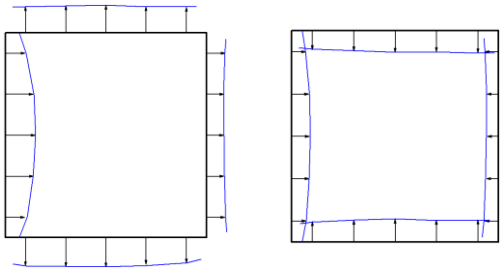

a. Mean b. Rms

Fig. 14 Mean and fluctuating wind pressure coefficients

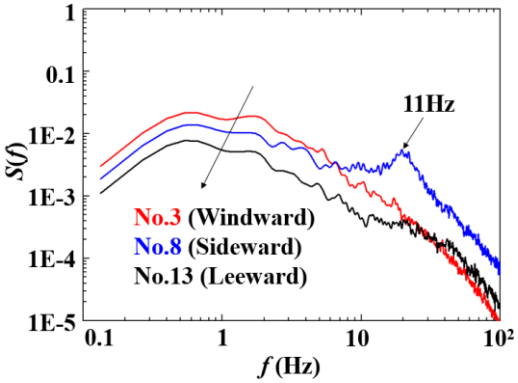

Fig. 15 PSD of the fluctuating wind pressure coefficients

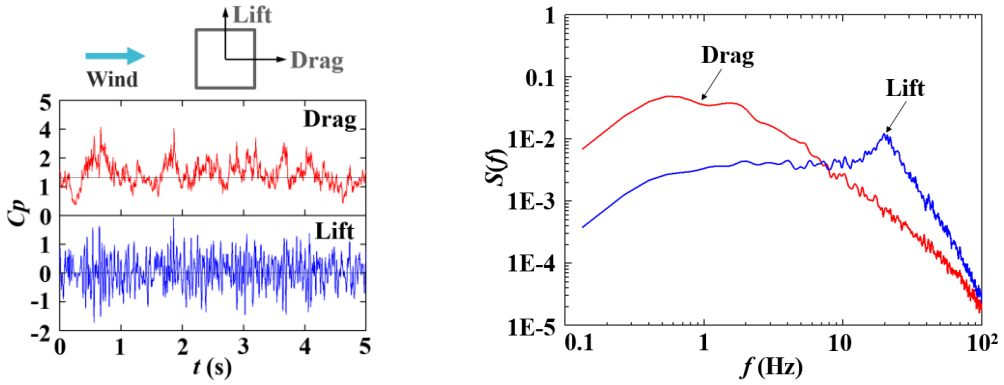

(a) Time history (b) PSD

Fig. 16 Drag force and lift force of the 7th layer of high-rise building

3.2.3 Covariance matrix-branched proper orthogonal decomposition

With previous understanding and knowledge about physical causes or behavior of bluff body flows, it is appropriate to think that the low-order covariance modes can characterize and represent for the known physical cause, phenomenon as well as these dominant modes with the high energy contribution can be associated with the bluff body flow pattern on the model surface.

Eigenvalues and eigenvectors corresponding to each covariance modes have been determined from covariance matrix of the fluctuating pressures. Fig. 17 shows first six covariance modes.

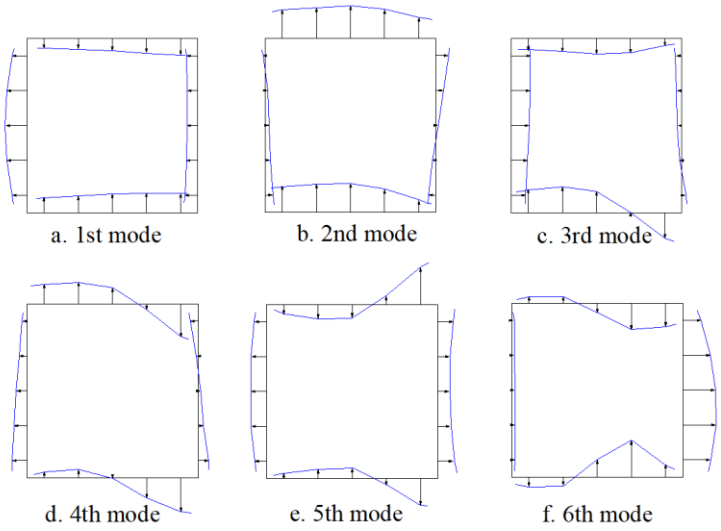

Fig. 17 First six covariance modes of experimental model

The 1st mode is symmetric corresponding to the drag force, with 39% energy. The 2nd mode is antisymmetric corresponding to the lift force, with 32% energy. Energy of the lowest two covariance modes of the fluctuating pressure fields is 71%. Obviously, the lowest two covariance mode contributes dominantly to the random pressure fields.

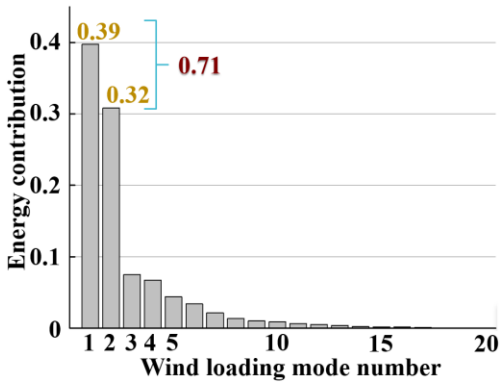

Fig. 18 Energy contribution of each covariance mode

Covariance principal coordinates associated with the covariance modes to build up the original pressure field has been determined from the measured fluctuating pressure. It is noted that the covariance principal coordinates are time-dependent uncorrelated processes.

The first and the second covariance principal coordinates corresponding to the drag force and the lift force, respectively, for both the time history and the power spectrum. It is noteworthy that only the first and the second covariance principal coordinates express considerable amplitudes, whereas the amplitudes of the other coordinates are small and inconsiderable. In the aspect of power spectrum, furthermore, the first and the second covariance coordinates not only dominate in their power spectral densities but they also contain all frequency characteristics of the physical causes of the random pressure field, whereas the other coordinates do not contain these frequencies.

Thus, it can be commented that the first and the second covariance modes and associated principal coordinates play important role in the description and identification of the random pressure field due to their dominant energy contribution and frequency containing of hidden physical events of the random pressure field.

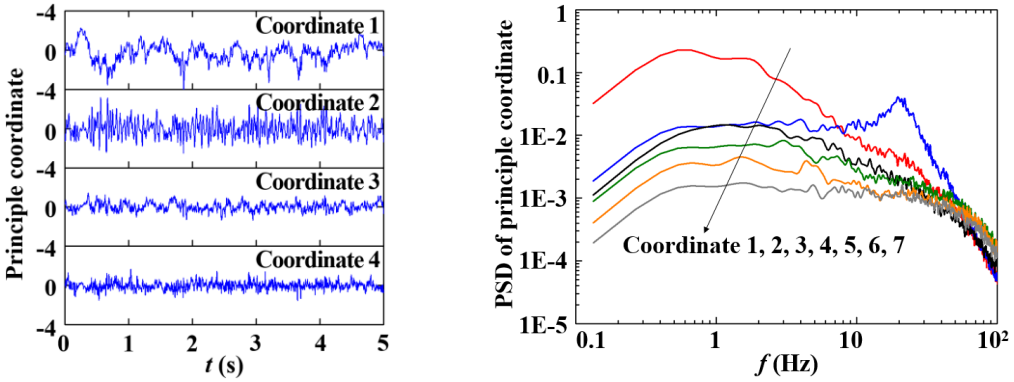

a. Covariance principle coordinate PSD of covariance principle coordinate

Fig. 19 Covariance principle coordinate

The original pressure fields can be reconstructed by using limited number of the low-order covariance modes or the low-order spectral modes. The reconstruction of original fluctuating pressure at Point 3 on the windward surface shows that, that reconstructed pressure time series using the first mode is similar to the original pressure. While the reconstruction of original fluctuating pressure at Point 8 on the sideward surface shows that, reconstructed pressure time series using the first two modes is similar to the original pressure, especially its contribution portion contains the frequency peaks can be used to identify hidden characteristics and physical phenomena of the original pressure.

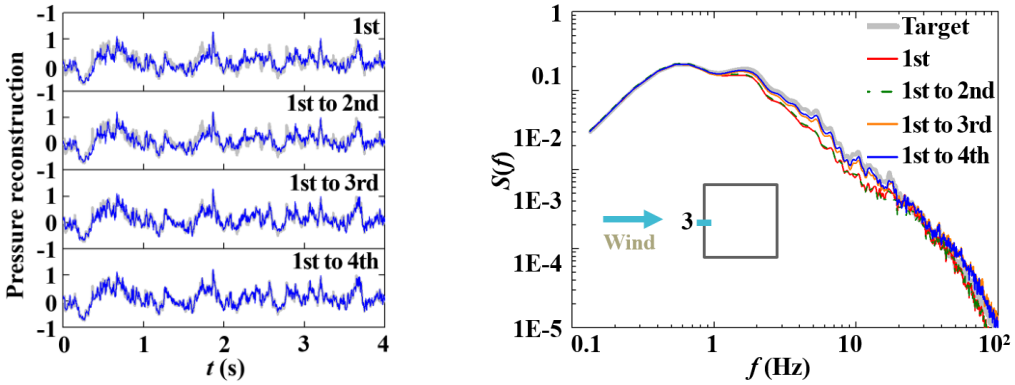

(a) Time history Recostructed PSD

Fig. 20 Reconstructed time history and PSD of P3

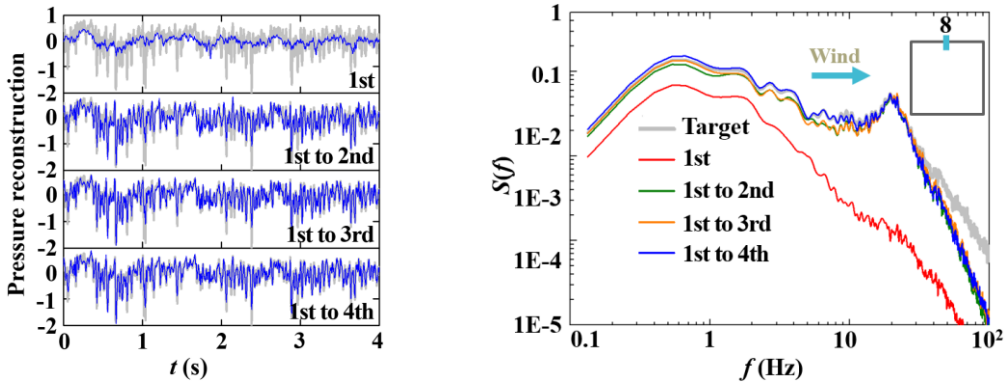

Time history Recostructed PSD

Fig. 21 Reconstructed time history PSD of P8

3.2.4 Spectral matrix-branched proper orthogonal decomposition

Energy contributions of the spectral eigenvalues (Fig. 22) show that, the first spectral modes contribute dominantly on the energy of the pressure fields, which contains 66% energy. This suggests that the first spectral mode may express the solution of the first two covariance modes, because of the similar energy contribution of the first spectral mode and the first two covariance modes. Accounted for the first two spectral modes, the contribution is 80%.

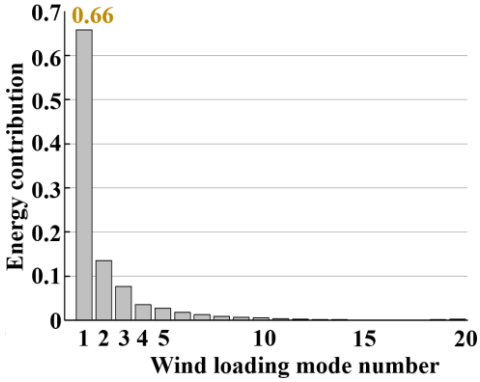

Fig. 22 Energy contribution of each spectral mode

Frequency-dependent spectral eigenvalues and spectral eigenvectors can be solved out from frequency-dependent cross spectral matrix of the random pressure field. Fig. 23 shows the first six spectral eigenvalues. The first spectral eigenvalues exhibit much dominantly than the others. The first spectral principle coordinate contain the frequency peak of the physical causes of the random pressure fields, whereas the others do not hold these frequency peaks.

From the spectral principle coordinates (Fig. 24), we can see the first spectral coordinate is dominant. It not only include the low frequency energy, but also has a peak in the high frequency range. Thus, the first spectral mode include both the two

mechanisms, which are the drag force and the lift force.

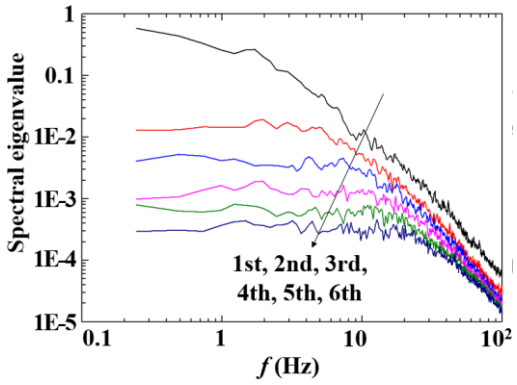

Fig. 23 First six spectral eigenvalues

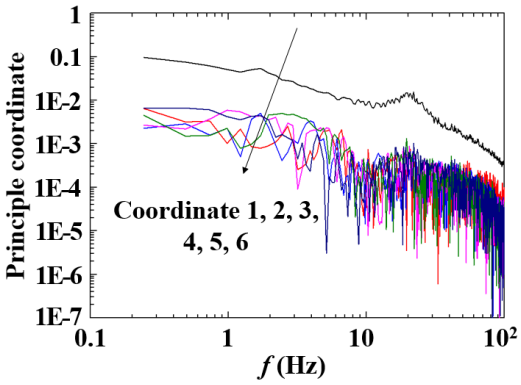

Fig. 24 First six spectral principle coordinates

The first spectral mode is shown in (Fig. 25(a)). To observe more easily, windward, sideward and leeward are shown respectively. On the windward and leeward side, the spectral modes are symmetric. On the sideward, the power spectrum in the high frequency range is increasing along the wind direction.

For the second spectral mode, on the windward and leeward sides, spectral modes are symmetric too. On the sideward, the spectrum in the low frequency range decrease along the wind direction, and the power spectrum in high frequency range increase along the wind direction.

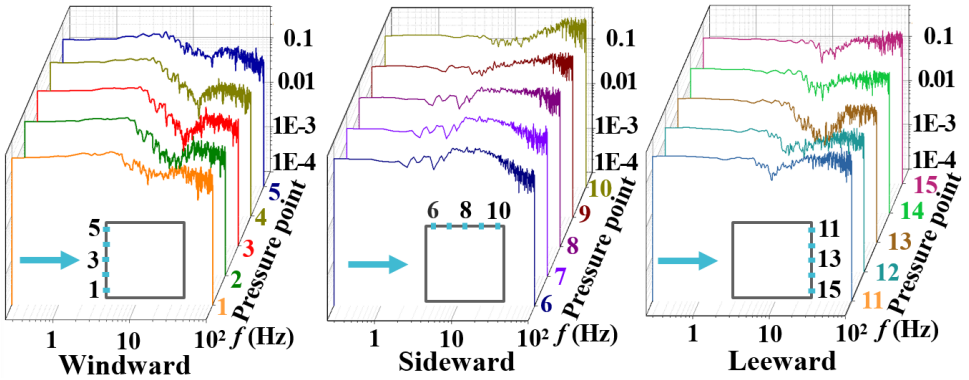

(a) Mode 1

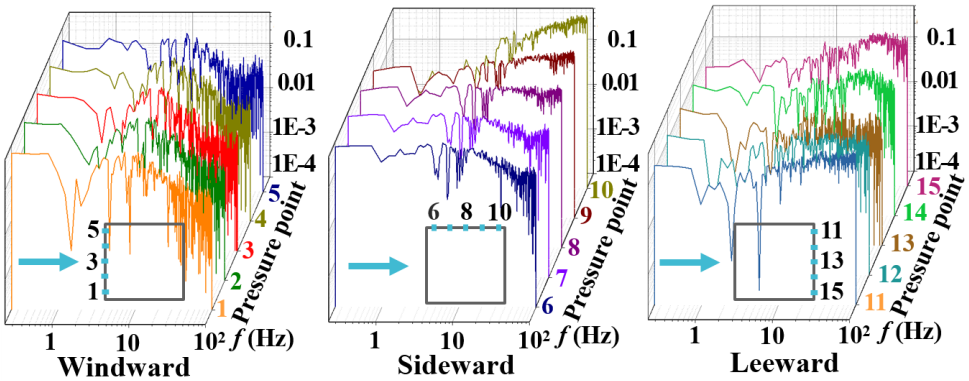

(b) Mode 2

Fig. 25 Spectral modes

The original pressure fields can be reconstructed by using limited number of the low-order covariance modes or the low-order spectral modes. The reconstruction of the PSD of original fluctuating pressure at Point 3 on the windward surface and Point 8 on the sideward surface shows that, only the first spectral mode are enough for reconstruction and identification of the pressure fields. At Point 3 on the windward

surface, the first spectral mode shows good agreement with the first covariance mode in reconstructing the original pressure. At Point 8 on the sideward surface, however, the first spectral mode exhibit better than the first covariance mode in reconstructing the original pressure at all frequency range.

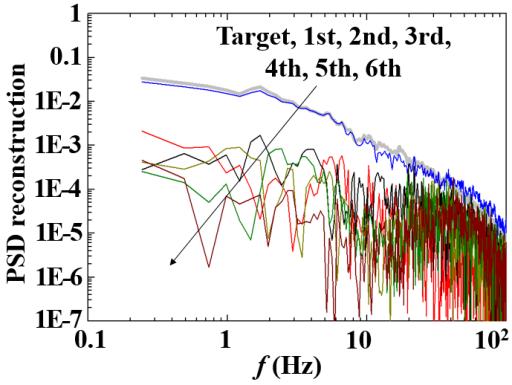

(a) Reconstructed spectrum of P3 from each mode

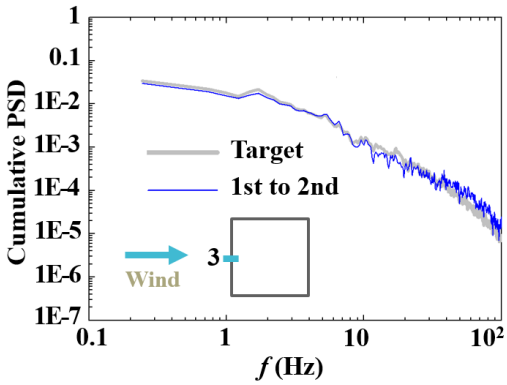

(b) Reconstructed spectrum of P3 from each mode

Fig. 26 Reconstructed spectrum of P3 each mode

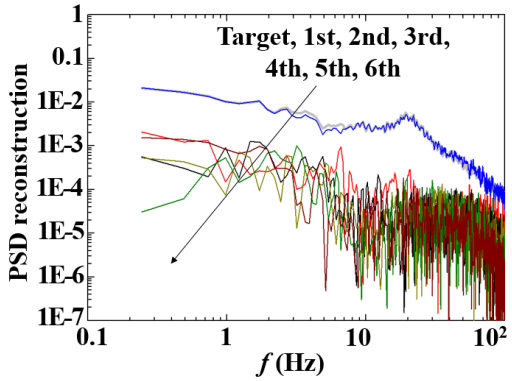

(a) Reconstructed spectrum of P8 from each spectral modes

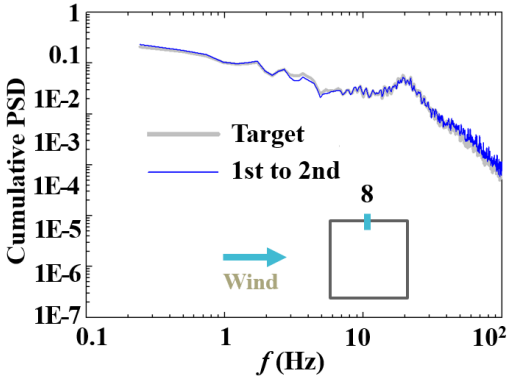

(b) Reconstructed spectrum of P8 from the first two spectral modes

Fig. 27 Reconstructed spectrum of P8 from the first two modes

3.3 Conclusions

For the flat-roof low-rise building:

Based on the covariance POD, the first two covariance modes are dominant, the reconstructed PSD of the original fluctuating pressure from the first covariance mode is lack of the energy in high frequency range. Based on the spectral POD, the first spectral mode is dominant, the reconstructed PSD of the original fluctuating pressure from the first spectral mode shows good agreement with the original PSD at all frequency range.

For the square-section high-rise building:

Based on the covariance POD, the first two covariance modes are dominant. Covariance modes corresponding to drag force and lift force can be identified. However, the reconstructed PSD of the original fluctuating pressure from the covariance modes is lack of the energy in high frequency range. Based on the spectral POD, the first spectral mode is dominant. The first spectral mode can reflect both the drag force and the lift force. Moreover, the reconstructed PSD of the original fluctuating pressure from the first spectral mode shows good agreement with the original PSD in all frequency range.

4. Published Paper etc.

[Underline the representative researcher and collaborate researchers]

[Published papers]

1. None

[Presentations at academic societies]
1. None

[Published books]
1. None

[Other]
Intellectual property rights, Homepage etc.

5. Research Group
1. Representative Researcher
Qingshan, Yang
2. Collaborate Researchers
1. Yong Chul, Kim
2. Yukio, Tamura
3. Wenshan, Shan

6. Abstract (half page)

Research Theme: Research on Proper Orthogonal Decomposition (POD) of wind pressures on hip-roof buildings
Representative Researcher (Affiliation): Qingshan, Yang (Chongqing University)
Summary・Figures
(To summarize briefly, only the results of high-rise building have been shown)
Analysis and identification of the fluctuating pressure field of the square section of the high-rise building using both the covariance matrix-based and spectral matrix-based proper orthogonal decompositions have been presented.
(1) Based on the covariance POD, the first two covariance modes are dominant. Covariance modes corresponding to the drag force and the lift force can be identified. However, the reconstructed PSD of the original fluctuating pressure from the covariance modes is lack of the energy in high frequency range.
(2) Based on the spectral POD, the first spectral mode is dominant. The first spectral mode can reflect both the drag force and the lift force. Moreover, the reconstructed PSD of the original fluctuating pressure from the first spectral mode shows good agreement with the original PSD in all frequency range.